

Supplement Material

On-line Data Supplement

Development of Aerobic Rat Model System

Rat models were founded from the genetically heterogeneous N:NIH population (80 males and 88 females) obtained from the National Institutes of Health (USA) in 1996¹. We developed the Low Capacity Runner (LCR) rats and High Capacity Runner (HCR) rats using two-way artificial selective breeding for intrinsic aerobic running capacity as described in detail previously.^{3, 4} Twenty-six mating pairs were randomly assigned from the 13 lowest and 13 highest capacity males and females to create 13 base families of LCR and HCR. At each subsequent generation, all offspring were tested for intrinsic running capacity at 11 weeks of age and the phenotypically “best” male and female offspring were selected from each family (within family selection) and became breeders for the next generation. A prearranged schedule of rotational matings was followed to yield retention of genetic variation and thus increases the overall response to selection⁵. After twenty generations of selection (n = 7,342 rats), HCR rats ran 1.2 km further on a test for maximal running distance than LCR rats, which is equivalent to running times of 63.4 ± 6 min vs. 20.4 ± 4 min, respectively (**Supplement Figure IA**).

Estimation of genetic parameters and breeding values.

We estimated the genetic parameters for the logarithm of distance and body weight using bivariate analyses with the “animal model”^{6,7}. For both traits, the model⁸ was

$$y_i = Fixed + A_{D,i} + A_{M,dam(i)} + E_C + e_i,$$

where *Fixed* includes correction factors treated as fixed effect, $A_{D,i}$ represents the additive genetic direct effect of the individual producing the record, $A_{M,dam(i)}$ represents the additive genetic maternal effect of the mother of the individual producing the record, E_C represents the non-genetic environmental effect common to individuals born in the same litter (the so-called common-environment effect⁹ and e_i represents the residual. We treated the direct and maternal genetic effects and the common environment effect as random effects. Hence, the variance due to those effects was estimated. The correlation between direct and maternal genetic effects was estimated as well. Common-environment effect explained 11% of phenotypic variance in distance, and 5% of phenotypic variance in body weight ($\sigma_{E_C}^2 / \sigma_y^2$ was 0.11 and 0.05 respectively).

The correction factors used in *Fixed* were

$$Fixed = line + generation + gender + litter\ size + best\ trial + operator + bF,$$

where *line* represents the genetic line, *generation* the generation to which the individual belongs, *gender* the gender of the individual, *litter size* the size of the litter in which the individual was born, *best trial* the trial number (1-5) in which the individual ran the greatest distance, *operator* the person performing the experiment, and *bF* the linear effect of the inbreeding coefficient of the individual. (We omitted the factor *best trial* from the model for body weight). We estimated fixed effects and variance components using restricted maximum likelihood (ReML;¹⁰ as implemented in the ASREML software¹¹. All correction factors in *Fixed* were significant.

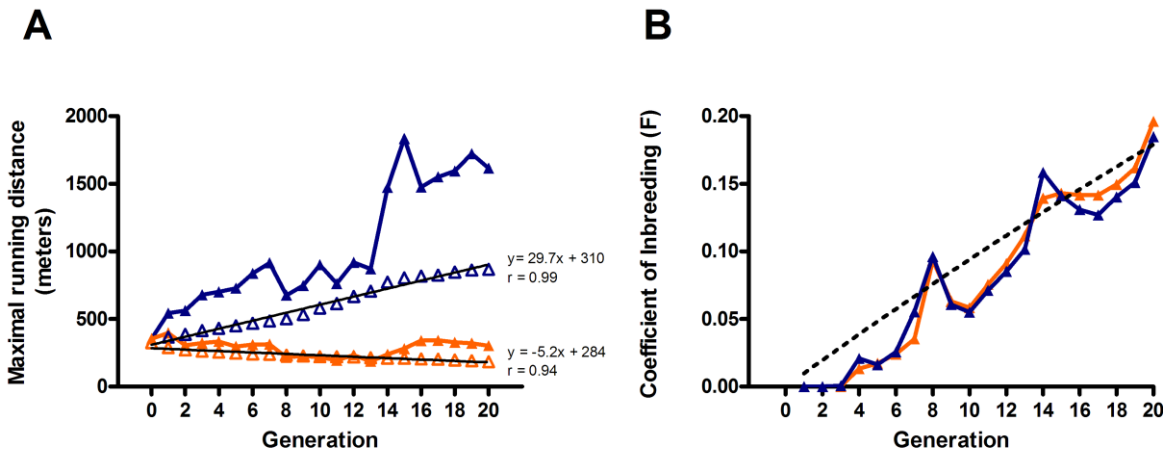
At generation 20, the genetic merit between the LCR and HCR populations differed by 4.7 fold, which reflects a 32% direct heritability, 11% maternal heritability, and a 20% realized heritability ($h^2 = 0.20$) for the trait of intrinsic (untrained) aerobic running capacity (**Online Table I**). In view of the fact that body weight and exercise capacity can be associated, it was not surprising there was a moderate negative correlation between the direct genetic effects on distance run and body weight ($r_g = -0.23$; $P < 0.005$; **Online Table II**).

Estimation of inbreeding (F)

We calculated the “predicted lowest possible inbreeding” using the exact relationship for rate of inbreeding⁹ defined as $\Delta F = 1/(2Ne) = 1/(4N-2)$. That is, when the number (N) of male and female breeders are chosen equally from all families, the effective number of breeding individuals (Ne) = $(2N-1) = 51$. Thus with 26 parents (13 families in each selected line), the exact expected inbreeding at generation 20 equaled $F_{20} = 1 - (1 - \Delta F)^{20} = 1 - (1 - 1/102)^{20} = 0.1788$, corresponding to a retention of 82.12% of the genetic heterogeneity of the founder parents. We estimated co-ancestries (f) retrospectively using the tabular method^{2,9} in which the inbreeding of individual X is computed from the basic ruling of

$$F_X = f_{PQ} = \frac{1}{4}(f_{AC} + f_{AD} + f_{BC} + f_{BD})$$

where: P and Q are the parents of X; A and B are the parents of P; and C and D are the parents of Q. After 20 generations of selection, both lines had F values close to the exact expected inbreeding estimate of $F = 0.1788$ (**Online Figure IB**).



Online Figure I. A contrasting rat model system was developed by two-way artificial selection for intrinsic (untrained) treadmill endurance running capacity. **(A)** Response to selection for Low Capacity Runners (LCR; orange) and High Capacity Runners (HCR; blue) across 20 generations ($n = 7,342$ rats) produced divergent rat populations with a 4.7 fold difference in maximal running distance (meters). Total estimated breeding values (EBV; open symbols with best fit line) represent the effect of genotype on the population mean. **(B)** Plotted are the estimated coefficients of inbreeding (F) across 20 generations for LCR (orange) and HCR (blue) rats. Values for F were calculated by a pedigree analysis based upon co-ancestries using the tabular method² and yielded a value of 0.196 for the LCR and 0.185 for the HCR rats at generation 20. For reference, the dotted line shows the exact expected inbreeding estimate calculated prospectively based upon the within family rotational breeding structure we employed.

Online Methods

All breeding and experimental procedures were approved by the Institutional Animal Care and Use Committees at the University of Michigan, Ann Arbor and the Norwegian University of Science and Technology.

Speed-ramped treadmill running test

Exercise capacity was assessed by a speed-ramped treadmill running test to exhaustion as previously described³. Briefly, each rat was tested for maximal endurance running capacity on five consecutive days using a speed-ramped running test on a motorized treadmill (Columbus Instruments, Columbus, OH) patterned after clinical stress tests. Exercise was performed at 15 degree incline. Treadmill speed started at 10 meters per minute and automatically increased 1 meter per minute every two minutes. For each rat, the single best maximal running distance (meters) of the five trials was used as the estimate of intrinsic aerobic endurance capacity.

VO_{2max}

VO_{2max} was measured with rats running uphill (25° inclination) on an enclosed treadmill chamber as previously described in detail¹². Because rats with significantly different body weights were compared, oxygen uptake (VO_2) was expressed in relation to body mass raised to the power of 0.75¹³.

Blood pressure

Blood pressure was measured using a non-invasive tail-cuff monitor (NIBP-8, Columbus Instruments, Columbus, OH). Animals were adapted to the blood pressure apparatus over 4 x 40 minute-sessions prior to testing. The average of 10 consecutive measurements was taken as a representative pressure for each animal.

Echocardiography

Global ventricular function was assessed by echocardiography (30MHz, Vevo 770, VisualSonics, Toronto, Canada) during 2% isoflurane/98% oxygen anesthesia.

Physical Activity and Energy Expenditure

VO_2 and carbon dioxide production (VCO_2) and spontaneous activity were recorded using a Comprehensive Laboratory Animal Monitoring System (CLAMS, Columbus Instruments), an integrated open-circuit calorimeter equipped with an optical beam activity monitoring device. The experimentation room was set at 20-23 °C with 12-12 hours (6:00PM~6:00AM) dark-light cycles. Rats were individually placed into the sealed chambers (12.25" x 7.38" x 7.25") with free access to food and water and measured continuously for 48~72 hour. VO_2 and VCO_2 in each chamber were sampled sequentially for 5 seconds in a 10 minutes interval and the motor activity was recorded every second from photo beam detection of horizontal (X) and vertical (Z) movements. Because LCR and HCR rats differ for body size and adiposity, we also indexed VO_2 to allometrically scaled body mass and lean body mass^{14, 15}. Respiratory quotient (RQ) was calculated as VCO_2/VO_2 . Home cage activity was measured using a precision balance¹⁶. Non-invasive estimates of body composition were measured using an NMR-based analyzer (Minispec LF90II, Bruker Optics, Billerica, MA). These measures were conducted by the University of Michigan Animal Metabolic Phenotyping Core.

Cardiomyocyte Cell Function

Single cardiomyocytes from the left ventricle were isolated with a Krebs–Henseleit Ca^{2+} -free buffer and collagenase type 2 (optimal exposure for each group) with $CaCl_2$ subsequently added stepwise to 1.8 mmol/L. Fura-2/AM-loaded (2 μ mol/L, Molecular Probes, Eugene, OR) cardiomyocytes were stimulated by bipolar electrical pulses at 5 Hz, whereby contractility was recorded by video-based sarcomere spacing (SarcLenTM, IonOptix, Milton, MA) and Ca^{2+} -handling was recorded by counting 510 nm emission after exciting with alternating 340 and 380 nm wavelengths on an inverted custom-made

fluorescence microscope (Cairn Research, Kent, UK) in a normal physiological HEPES-based solution (1.8 mM Ca^{2+} , 37° C). In separate Fura-2/AM-loaded cells, caffeine-induced Ca^{2+} release was measured to assess sarcoplasmic reticulum Ca^{2+} load, whereas caffeine application after a 40-second quiescent period with 0 Na^+ and 0 Ca^{2+} in the extracellular solution and in the presence and absence of the ryanodine receptor blocker tetracaine was used to assess sarcoplasmic reticulum Ca^{2+} leak. Fura-2 signals were subsequently analyzed using Ionoptics analyzing program version 5.0 (IonOptix). The ratio signal of the two excitation wavelengths was converted to $[\text{Ca}^{2+}]_i$ by measuring R_{\min} (0.48 ± 0.06) and R_{\max} (6.4 ± 0.8) in permeabilized cells and assuming a K_d of 200 nM. Contractility and Ca^{2+} handling were measured in 6 cardiomyocytes/rat and analyzed from 10 consecutive contractions after stabilization. Cell dimensions (length and width) in quiescent cardiomyocytes were determined from widefield images of 150 cells in each animal using a calibrated caliper.

Confocal Imaging for Calcium sparks and T-tubule Density

Quiescent cardiomyocytes loaded with Fluo-3/AM (10 μM , Molecular Probes) were confocal line scanned in physiological HEPES-based solution (1.8 mM Ca^{2+} , 37° C) to measure Ca^{2+} sparks. Excitation was provided by a 488 nm laser, whereas 505-530 nm emission was collected with a photomultiplier tube (Zeiss LSM 510, Jena, Germany). A line along the length of the cell set to exclude nuclei was continuously fast-scanned, whereupon Ca^{2+} sparks were subsequently counted and characterized using automated detection and measurement algorithms: 6 cardiomyocytes/rat were studied. Quiescent, non-perfused cardiomyocytes were also loaded with the membrane specific Di-8-ANEPPS dye (10 μM , Molecular Probes) and confocal Z-stack frame scanned with a 1 μm Z-step between each image in order to study transverse (T)-tubules, with the optical parameters as described above. 10 images/cell in 6 cardiomyocytes/rat were captured from the middle of each cell and analyzed with custom-made applications in IDL 6.0 (ITT Visual, Boulder, CO) to measure the relative density of T-tubules. From each image, we counted pixels stained with the dye relative to the total number of pixels after removing pixels associated with the non-T-tubular plasma membrane or pixels outside the boundary of the cell. This enabled a quantification of the relative T-tubule density normalized to cell size from each individual cardiomyocyte.

Molecular Assays

Analysis of PGC-1 α , UCP2, and TAS (total antioxidant status) were performed as previously described^{4, 17}. Briefly, left ventricular tissue was homogenized in ice-cold lysis buffer (150 mM NaCl and 50 mM HEPES including protease inhibitors, pH 7.6). Equal amounts of homogenate were subjected to SDS PAGE and Western blot analysis with goat polyclonal antibodies against PGC-1 α (K-15) and UCP2 (N-19), both purchased from Santa Cruz Biotechnology (Santa Cruz, CA). To normalize for the amount of proteins on the gel, proteins were re-probed with a monoclonal antibody against α -actin (Sigma, St. Louis, MO). Proteins were then detected by enhanced chemiluminescence and quantified by densitometry. TAS in plasma was measured by photometry on a Cobas Mira S Analyzer by an enzymatic assay according to manufacturer's specifications (TAS, Randox Laboratories Ltd., Crumlin, UK). Blood chemistries and serum levels were determined from blood collected by either saphenous vein or tail snip methods and analyzed by University of Michigan Pathology Core facilities. Using 96-well plate-format assays, we profiled the production of multiple cytokines simultaneously in a single sample. Serum cytokine profiling was performed at Johns Hopkins University using bead-based multiplex assay (BioRad, Hercules, CA) according to the manufacturer's instructions, as described previously¹⁸. The panel included pro-inflammatory (IL-6, TNF- α , IL-1 α , IL-1 β , IL-2, IFN- γ , GM-CSF) and anti-inflammatory (IL-10, IL-4) cytokines.

OnlineTable I. Heritabilities in LCR and HCR rats

Trait	Estimate
log-distance, direct ^a	0.32 ± 0.04
log-distance, maternal ^b	0.11 ± 0.04
Body weight, direct	0.49 ± 0.04
Body weight, maternal	0.05 ± 0.03
log-distance, realized ^c	0.20 ± 0.03

Direct heritability is the direct additive genetic variance, expressed as a proportion of phenotypic variance,

$$h_D^2 = \sigma_{A_D}^2 / \sigma_y^2.$$

^bMaternal heritability is the maternal additive genetic variance, expressed as a proportion of phenotypic variance,

$$h_M^2 = \sigma_{A_M}^2 / \sigma_y^2.$$

^cRealized heritability is the regression coefficient of trait value in the next generation on mean phenotype of the selected parents; it represents the response to selection expressed as a proportion of the phenotypic selection

differential. For a maternally affected trait, realized heritability equals $h_R^2 =$

$$(\sigma_{A_D}^2 + 1.5\sigma_{A_{DM}}^2 + 0.5\sigma_{A_M}^2) / \sigma_y^2.$$

OnlineTable II. Estimated genetic correlations of LCR and HCR rats

Trait	Dm	Bd	Bm ^a
log-distance, direct	-0.63 ± 0.11	-0.23 ± 0.08	
log-distance, maternal (Dm)		-0.24 ± 0.14	-0.11 ± 0.30
Body weight, direct (Bd)			0.71 ± 0.29

^aBm = body weight, maternal.

Online Table III. Echocardiographic evaluation of old age LCR and HCR rats.

	LCR n = 5	HCR n = 5	P-value
Heart rate (beats/min)	359±21	339±13	NS
LVESD (mm)	4.6±0.4	5.7±0.3	<0.05
LVEDD (mm)	7.5±0.4	7.5±0.5	NS
LVESV (μl)	106±28	139±23	<0.05
LVEDV (μl)	323±49	311±59	NS
SV (μl)	217±35	172±53	NS
FS (%)	38.2±5.2	23.6±4.8	<0.05
EF (%)	67±6	54±8	<0.05
E (mm/s)	611±95	994±120	<0.05
A (mm/s)	673±169	700±149	NS
E/A ratio	0.9±0.1	1.5±0.5	<0.05
IVRT (ms)	27.3±3.1	24.3±1.2	NS
E' (mm/s)	32.3±2.2	39.4±1.2	<0.05
A' (mm/s)	49.7±5.3	35.5±2.3	<0.05
E'/A' ratio	0.7±0.1	1.1±0.1	<0.05
S' (mm/s)	32.6±3.1	27.2±3.6	<0.05

LVESD, LVEDD, left ventricle end systolic and diastolic diameter; LVESV, LVEDV, left ventricle end systolic and diastolic volume; SV, stroke volume; FS, fractional shortening; EF, ejection fraction; E, early diastolic transmitral flow velocity; A, atrial systolic transmitral flow velocity, E/A, ratio of E to A; IVRT, isovolumic relaxation time; E', early diastolic myocardial relaxation velocity; A', myocardial velocity during atrial contraction; E'/A', ratio of E' to A'; S', systolic myocardial velocity. Data were expressed as mean±/SD.

OnlineTable IV. Age-related lesions between LCR and HCR rats as determined by

Lesion	LCR			HCR		
	# with lesions	% with lesions	Severity of lesion Mean (SD)	# with lesions	% with lesions	Severity of lesions Mean (SD)
Adrenal: cortical degeneration	12/29	41.4%	1.8 (1.0)	29/53	54.7%	1.9 (0.9)
Kidney: chronic progressive nephropathy	10/29	34.5%	2.7 (1.4)	28/53	52.8%	2.4 (1.4)
Muscle: degeneration/regeneration	4/29	13.8%	1.8 (0.96)	17/53	32.1%	1.4 (0.6)
Lung : foam cell foci	6/29	20.7%	1.2 (0.59)	17/53	32.1%	1.4 (0.05)
Pituitary: adenoma/carcinoma	8/29	27.6%	1/8 carcinoma	9/53	17.0%	2/9 carcinoma
Heart: fibrosis	4/29	13.8%	1.8 (0.96)	5/53	9.4%	1.6 (0.5)
Liver: lipidosis	2/29	6.9%	2.0 (1.4)	2/53	3.8%	2.0 (1.0)

^aThe entire range of lesions was observed and an arbitrary scale set from 0 (no lesion) to +4 for the most severe lesion in this study.

Online Table V. Blood chemistry profiles obtained from aged low and high aerobic capacity rats.

Marker	(Normal range)	LCR Mean (SD)	n	HCR Mean (SD)	n	P value
Triglycerides,mg/dL	(26 -108)	140 (52)	28	86 (45)	20	<0.001
ALT, U/L	(94 - 103)	91 (32)	29	124 (52)	25	0.005
Glucose, mg/dL	(50 -135)	102 (26)	30	89 (21)	25	0.05
Total Protein, g/dL	(5.3 - 6.9)	7.8 ± 1.1	29	8.0 (0.8)	22	0.51
Albumin, g/dL	(3.8 - 4.8)	3.9 ± 0.8	29	4.2 ± 0.7	22	0.25
Globulin, g/dL	(1.5 -2.8)	3.9 ± 0.5	29	3.8 ± 0.3	22	0.59
ALKP, U/L	(120 - 176)	75 ± 38	29	89 ± 46	25	0.26
AST, U/L	(80 - 167)	225 ± 148	28	307 ± 226	22	0.13
SGGT, U/L	(2.4 – 5.7)	4.5 ± 13.9	26	5.6 ± 21.9	16	0.85
Total Bilirubin, mg/dL	(1.5 - 4.2)	2.4 ± 3.6	29	3.4 ± 5.5	25	0.39
Cholesterol, mg/dL	(20 - 92)	108 ± 59	30	97 ± 41	25	0.42
Amylase,,IU/L	(326 -2246)	1271 ± 455	29	1362 ± 466	25	0.47
BUN, mg/dL	(4.2 - 19.1)	16.6 ± 4.7	30	17.6 ± 3.2	25	0.37
Creatinine, mg/dL	(1.1 - 1.7)	0.3 ± 0.1	30	0.3 ± 0.2	25	0.27
CK, U/L	(48 - 340)	617 ± 285	28	647 ± 364	22	0.74
Calcium,mg/dL	(5.3 - 11.6) mg/dL)	9.8 ± 1.7	29	9.6 ± 2.0	25	0.68

Abbreviations ALT, Alanine Aminotransferase;ALKP, Alkaline Phosphatase AST, Aspartate Aminotransferase; SGGT,Serum Gamma-Glutamyl Transferase; BUN, Blood Urea Nitrogen;CK,Creatine Phosphokinase

OnlineTable VI. Cytokine panel comparison between LCR and HCR rats as determined by bead-based multiplex assay

Cytokine marker pg/ml	LCR^a Mean(SD)	HCR^a Mean(SD)	P value
TNF- α	223.5 (104.3)	33.96 (31.74)	< 0.001
GM-CSF	355.6 (43.68)	238.1 (66.59)	< 0.001
IL-4	543.5 (52.69)	411.2 (117.2)	0.007
IL-10	1881 (742.4)	1192 (580.1)	0.043
IL-1 β	1455 (608.3)	1083 (589.9)	0.21
IL-1 α	5.791 (8.509)	46.31 (133.2)	0.38
IL-6	6500 (634.8)	6224 (1158)	0.54
IFN- γ	111.0 (54.95)	84.88 (112.1)	0.54
IL-2	32090 (20320)	29050 (13360)	0.73
IL-4	543.5 (52.69)	411.2 (117.2)	0.007
IL-10	1881 (742.4)	1192 (580.1)	0.043

Abbreviations: TNF- α , tumor necrosis factor- α ; IL, Interleukin; IFN- γ , interferon; GM-CSF, granulocyte-macrophage colony-stimulating factor

^an = 9

References

1. Hansen C, Spuhler K. Development of the national institutes of health genetically heterogeneous rat stock. *Alcohol Clin Exp Res*. 1984;8:477-479
2. Plum M. Computation of inbreeding and relationship coefficients - in populations with a relatively small number of different male ancestors. *J Hered*. 1954;45:92-94
3. Koch LG, Britton SL. Artificial selection for intrinsic aerobic endurance running capacity in rats. *Physiol Genomics*. 2001;5:45-52
4. Wisloff U, Najjar SM, Ellingsen O, Haram PM, Swoap S, Al-Share Q, Fernstrom M, Rezaei K, Lee SJ, Koch LG, Britton SL. Cardiovascular risk factors emerge after artificial selection for low aerobic capacity. *Science*. 2005;307:418-420
5. Falconer DS. Genetic aspects of breeding methods. *The ufaw handbook on the care and management of laboratory animals*. Edinburgh: Churchill Livingstone; 1976:7-26.
6. Henderson CR. Estimation of genetic parameters. *Biometrics*. 1950;6:186-187
7. Kruuk LE. Estimating genetic parameters in natural populations using the "animal model". *Philos Trans R Soc Lond B Biol Sci*. 2004;359:873-890
8. Willham RL. Covariance between relatives for characters composed of components contributed by related individuals. *Biometrics*. 1963;19:18-&
9. Falconer DS, Mackay TFC. *Introduction to quantitative genetics*. Essex: Addison Wesley Longman, Ltd.; 1996.
10. Patterson HD, Thompson, R. Recovery of inter-block information when block sizes are unequal. *Biometrika*. 1971;58:545-554
11. Gilmour AR, Gogel, B.J., Cullis, B.R., Welham, S.J., Thompson, R. Asreml user guide release 3.0. 2009
12. Wisloff U, Helgerud J, Kemi OJ, Ellingsen O. Intensity-controlled treadmill running in rats: Vo(2 max) and cardiac hypertrophy. *Am J Physiol Heart Circ Physiol*. 2001;280:H1301-1310
13. Taylor CR, Maloiy GM, Weibel ER, Langman VA, Kamau JM, Seeherman HJ, Heglund NC. Design of the mammalian respiratory system. Iii scaling maximum aerobic capacity to body mass: Wild and domestic mammals. *Respir Physiol*. 1981;44:25-37
14. Batterham AM, George KP, Mullineaux DR. Allometric scaling of left ventricular mass by body dimensions in males and females. *Med Sci Sports Exerc*. 1997;29:181-186
15. Whalley GA, Gamble GD, Doughty RN, Culpan A, Plank L, MacMahon S, Sharpe N. Left ventricular mass correlates with fat-free mass but not fat mass in adults. *J Hypertens*. 1999;17:569-574
16. Biesiadecki BJ, Brand PH, Koch LG, Britton SL. A gravimetric method for the measurement of total spontaneous activity in rats. *Proc Soc Exp Biol Med*. 1999;222:65-69
17. Wisloff U, Stoylen A, Loennechen JP, Bruvold M, Rognmo O, Haram PM, Tjonna AE, Helgerud J, Slordahl SA, Lee SJ, Videm V, Bye A, Smith GL, Najjar SM, Ellingsen O, Skjaerpe T. Superior cardiovascular effect of aerobic interval training versus moderate continuous training in heart failure patients: A randomized study. *Circulation*. 2007;115:3086-3094
18. Abadir PM, Periasamy A, Carey RM, Siragy HM. Angiotensin ii type 2 receptor-bradykinin b2 receptor functional heterodimerization. *Hypertension*. 2006;48:316-322